

The use of nanostructured materials loaded with pH indicating molecules for corrosion sensing

I. Sousa, A. Kuznetsova, T. Galvão, J. Carneiro, M. Reyes, A. Bastos, J. Tedim, M.G.S. Ferreira
CICECO-Aveiro Institute of Materials, DEMaC University of Aveiro
Campus de Santiago
Aveiro, 3810-193
Portugal
joao.tedim@ua.pt

ABSTRACT

In this work we report the synthesis of different materials for immobilization of well-known pH indicators, to be used as additives in coatings for corrosion sensing: inorganic materials such as layered double hydroxides, silica nanocapsules and polymeric microcapsules (chitosan). The materials obtained were characterized by X-ray diffraction, Fourier transform infrared spectroscopy and scanning electron microscopies. Furthermore, the release profile of the obtained materials was performed using UV-Visible spectrophotometry under conditions relevant for the onset of corrosion processes, namely in the presence of NaCl and different pH conditions. The release and color changes were correlated with pH maps obtained by the scanning ion-selective technique for different galvanic couples (Al-Cu, Fe-Zn) and magnesium alloy AZ31. The results show that the materials obtained are able to change color, associated with the pK_a of selected indicators and ascribed to pH changes in the alkaline direction as result of cathodic activity in different metals. These findings open prospects for the use of the prepared additives in functional coatings for corrosion sensing.

Key words: Corrosion, pH indicator molecules, controlled release, layered double hydroxides, silica nanocapsules, chitosan microcapsules, sensors.

INTRODUCTION

Detection and mitigating actions are inter-related parts of the tackling of corrosion in a cost-effective way. Previous works available in the literature have shown the potential for using pH indicators as a simple and user-friendly approach for detection of corrosion activity

.¹⁻³ In fact, the association between the electrochemical processes occurring at the metal/solution interface, transduction into a measurable signal and correlation with level of degradation constitute an ever actual problem and challenge in the field of corrosion science and engineering.

In this work, we revisit the use of pH indicating molecules as active components of novel hosting structures for detection of corrosion.⁴ The designed systems encompass materials at micro and nanoscale with capacity for controlled release of substances, to be used as functional additives into polymeric coatings and thus impart self-sensing properties. The advantages associated with immobilization of pH indicators relatively to the direct addition of organic molecules into coating formulations can be the limitation of unwanted reactions between coating components and the pH indicators, and the localized nature of the response since only materials close to defects or sites where corrosion initiates will be signaled.

In the following sections the materials used in this work are summarily presented.

System I – Layered Double Hydroxides

Layered double hydroxides (LDHs), also known as anionic clay materials have been extensively reported for the intercalation and controlled release of different active species, from drug molecules⁵ to corrosion inhibitors.⁶ These materials may release the intercalating species by anion exchange or by dissolution under very acidic conditions. In the context of corrosion sensing, the main expected trigger for these materials is the presence of chloride species that will be exchanged with the intercalating species.⁷

System II – Silica Nanocapsules

Porous hollow silica materials occupy a prominent position in research science because of their easy preparation and potential applications in catalysis, adsorption/separation, sensing and active materials, which have made them very attractive in the past decade.^{8,9} Recently, the interest in these materials as carriers in controlled release has increased due to their several attractive features, such as stable uniform mesoporous structure, high surface area, tunable pore sizes and well defined surface properties. Furthermore, hollow silica spheres facilitate a high storage capacity and excellent sustained release properties due to their unique hollow core structures that act as reservoir for active molecules.^{8,9}

System III – Chitosan microcapsules

Chitosan is a linear copolymer of β -(1-4)-2-amido-2-deoxy-d-glucan (glucosamine) and β -(1-4)-2-acetamido-deoxy-d-glucan (N-acetylglucosamine) that can be produced from chitin by partial alkaline deacetylation. Chitin is the second most abundant polysaccharide in nature, after cellulose, and is available worldwide.¹⁰ Previous works have shown that chitosan is a good alternative as a protective coating against corrosion of metallic substrates, due to its good film-forming ability, superior adhesion to metallic surfaces and versatility associated with the easiness of chemical functionalization.¹⁰ The design and application of biopolymers as support for controlled release of species is currently one of the most important aspects in the development of active materials.

pH indicators

Due to the fact that phenolphthalein (PhPh, Figure 1) is colorless at a pH below 8.2 and turns to pink at pH higher than 8.2, it is currently one of the best options for corrosion sensing purposes. This characteristic can be useful to monitor the rise in pH associated with corrosion activity.⁴

Thymol blue (TB, Figure 1) is yellow at a pH below 8.0 and blue at pH higher than 9.6. In very acidic media, TB acquires a red color (pH < 1.2).¹¹

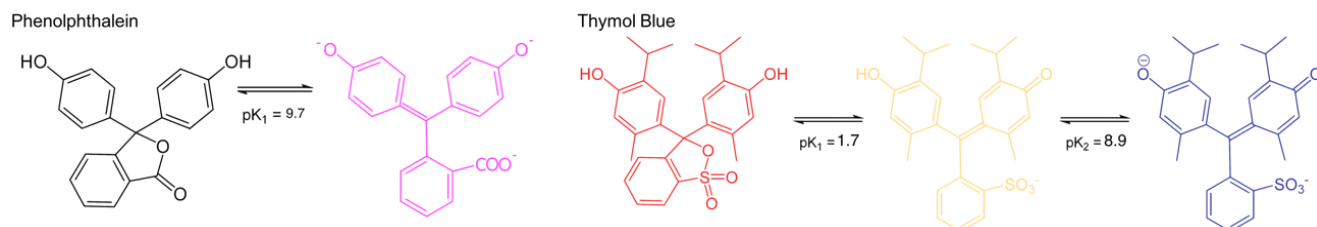


Figure 1: Phenolphthalein (left) and Thymol Blue (right) acid-base equilibrium.

EXPERIMENTAL PROCEDURE

Synthesis of layered double hydroxides

First, zinc-aluminum layered double hydroxides with the nitrate anion intercalated (Zn(2)Al-NO_3) were prepared by the co-precipitation route. The synthesized Zn(2)Al-NO_3 was calcined at $150\text{ }^\circ\text{C}$ during 3 h ($1\text{ }^\circ\text{C}\cdot\text{min}^{-1}$ ramp up and $10\text{ }^\circ\text{C}\cdot\text{min}^{-1}$ ramp down).

Then, PhPh was dissolved in ethanol (2.5 g of PhPh for 30 mL ethanol) and the calcined LDHs were immersed in this solution for 3 days at $60\text{ }^\circ\text{C}$.

The prepared material Zn(2)Al-PhPh , referred hereafter as LDH-PhPh, was filtrated and washed 2 times with sufficient amount of water (around 100 mL of water for both steps of washing for each type of LDHs), and the particles were dried in an oven at $60\text{ }^\circ\text{C}$ for 2 days. The materials were characterized by XRD.

Synthesis of silica nanocapsules

Synthesis of silica nanocapsules containing phenolphthalein (PhPh) was performed according to a published procedure.¹² Briefly, capsules were synthesized through an oil-in-water miniemulsion with ethyl ether and water as the oil and water phase, respectively, hexadecyltrimethylammonium bromide (CTAB) as a surfactant and tetraethyl orthosilicate (TEOS) as the silica precursor.

Synthesis of chitosan microcapsules

Chitosan (2.5 % w/v) was dissolved in a 5 % v/v acetic acid solution and stirred overnight to achieve complete dissolution. To 100 mL of chitosan solution, $\sim 0.15\text{ w/v\%}$ of thymol blue (TB) was added and stirred, until complete dissolution. The samples were then spray dried with spray-drying conditions of $180\text{ }^\circ\text{C}$ and $30/357\text{ mm/L}\cdot\text{h}^{-1}$ for inlet temperature and air flow, respectively.

Characterization techniques

Morphological characterization of the different capsules was performed on a Hitachi S4100 Scanning Electron Microscope* with an electron beam energy of 25 keV. Silica nanocapsules were sputtered with carbon while chitosan microcapsules were sputtered in Au/Pd.

Release studies were monitored by UV-Vis spectrophotometry on a Scan-Spec miniature UV-Vis spectrophotometer (ScanSci)†.

The powder XRD characterization at room temperature of the obtained materials was performed using a PANalytical X'Pert Powder diffractometer‡ (Ni filtered Cu $\text{K}\alpha$ radiation, a tube power of 45 kV and 40

* Trade name

† Trade name

‡ Trade name

mA) coupled with a PIXcell1D detector[§], and an exposition time of 6 s per step of 0.02° over an angular range (2θ) between 4 and 65°.

The AFM was carried out with a commercial AFM system (Veeco multimode with nanoscope III controller^{**}) under ambient conditions, collecting images in tapping mode.

Computational Details

The periodic model density functional theory (DFT) calculations were performed with the Quantum ESPRESSO^{††} code.¹³ All the molecular structure optimization details were performed as reported in a previous work,¹⁴ using the PBE exchange-correlation functional,¹⁵ ultrasoft pseudopotentials, cutoffs of 40 Ry and 240 Ry for the kinetic energy and charge density of the plane wave basis sets, respectively, and a 2 × 2 × 1 k-point mesh for the first Brillouin zone integrations. The optimization procedure was stopped after all the forces were lower than 10⁻³ Ry.

The periodic structure of bulk Zn(2)Al-PhPh was modelled by a (2√3 × 2√3)R30° supercell as described in detail in a previous work [14]. The structures of Zn(2)Al-NO₃, Zn(2)Al-OH and Zn(2)Al-CO₃ were also optimized for comparison, using the following supercells: [Zn₈Al₄(OH)₂₄](PhPh)₂·8H₂O, [Zn₈Al₄(OH)₂₄](NO₃)₄·8H₂O, [Zn₈Al₄(OH)₂₄](OH)₄·8H₂O and [Zn₈Al₄(OH)₂₄](CO₃)₂·8H₂O.

Substitution energies of NO₃⁻ in the precursor material by OH⁻, CO₂⁻ and PhPh²⁻, and adsorption energy of PhPh onto an Zn(2)Al cationic surface were also calculated in this work.

Characterization of metal substrates using SIET technique

The pH micropotentiometric electrodes were made in the laboratory. Single-barreled borosilicate glass capillaries with an outer diameter of 1.5 mm (WPI,USA, Ref. TW150-4^{††}) were thinned with a P97 micropipette puller (Sutter^{§§}, USA) using a four step pulling protocol giving a tip of 2 μm in diameter on one end. The micropipettes were silanized for 2 hours in an oven at 200 °C after injection of 200 μL of N,N-dimethyltrimethylsilylamine (Fluka, Ref. 41716^{***}). The micropipette was back-filled with 0.01 M KH₂PO₄ + 0.1 M KCl – internal solution and the cocktail column length at the tip is 25-30 μm column of hydrogen I cocktail B ionophore (Fluka, Ref. 95293^{†††}). It was then inserted in a half-cell plastic holder (WPI, USA, Ref.EHB1^{†††}) containing a chloridized silver wire as internal reference electrode. A homemade Ag/AgCl, 0.05 M NaCl electrode worked as external reference electrode. The microelectrode was mounted in the same 3D positioning system used for SVET. An IPA2 amplifier (input resistance >1015 W) manufactured by Applicable Electronics Inc.^{§§§} was controlled by the ASET^{****} program to measure and record the data. The microelectrodes were calibrated before and after measurements with commercial pH buffers (Riedel-de Haen^{††††}), giving a linear response in the 5 to 13 pH range (Figure 2).

§ Trade name

** Trade name

†† Trade name

‡ Trade name

§§ Trade name

*** Trade name

††† Trade name

‡‡ Trade name

§§§ Trade name

**** Trade name

†††† Trade name

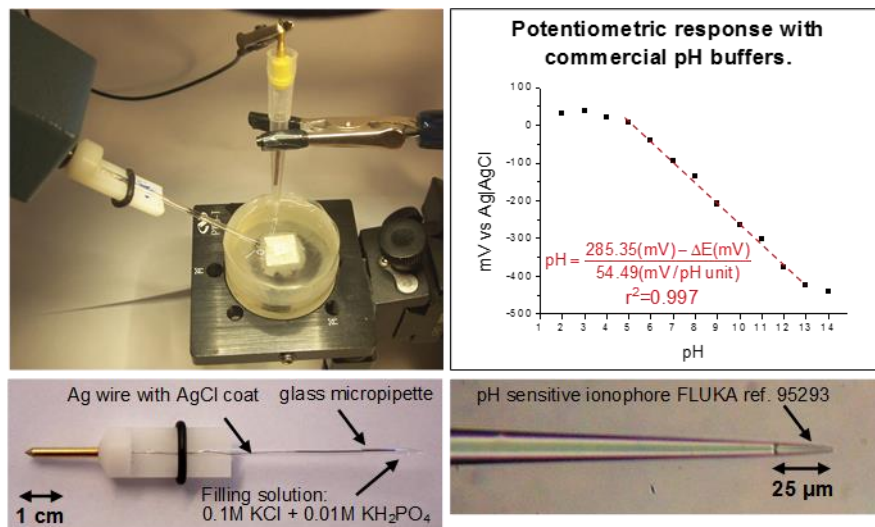


Figure 2: Ion selective microelectrode, potentiometric cell and potentiometric response.

The probe scanned 100 μm above the surface and maps comprised 35 x 35. In each measurement point the probe waited 1 s.

Samples

Two pairs of wires (Zn-Fe or Al-Cu) of 1 mm diameter were embedded separately in epoxy resin (EpoKwick, Buehler, USA^{###}). The Zn, Fe, Cu and Al wires were 99.99 % pure. The resulting samples were abraded with 1200 grade SIC paper and washed in distilled water followed by ethanol. After abrasion the samples depicted only two metallic disks in an insulating surface (Figure 3) and the wires were electrically connected in the backside. Adhesive tape around the epoxy holders served as solution container and the testing solution was 0.05 M NaCl (196 $\Omega\cdot\text{cm}$). A similar procedure was carried out to assemble a metal rod of magnesium alloy AZ31 in the epoxy resin.

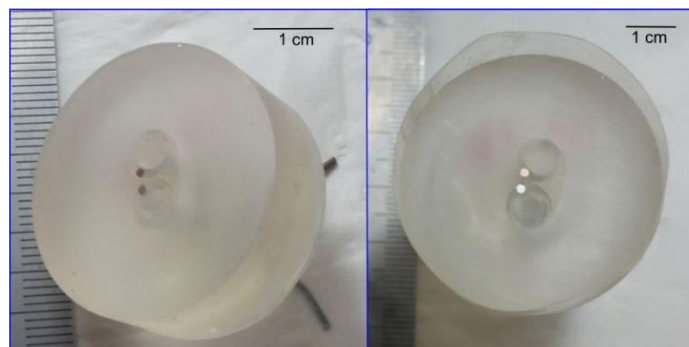


Figure 3: Samples for test.

RESULTS

Structure analysis of layered double hydroxides with phenolphthalein

In Figure 4 is presented an AFM image of the typical plate-like hexagonal morphology¹⁴ of the LDHs synthesized in this work.

^{###} Trade name

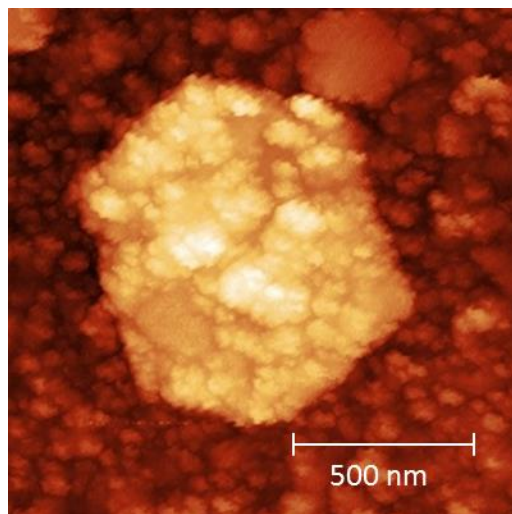


Figure 4: AFM image of typical LDH structure.

From the periodic model DFT calculations performed in this work for LDH-PhPh, it was predicted a (003) reflection around 5° . Analysing the experimental Zn(2)Al-PhPh XRD pattern (Figure 5) it is not possible to identify a peak around 5° , which means that PhPh was not intercalated in the interlayer.

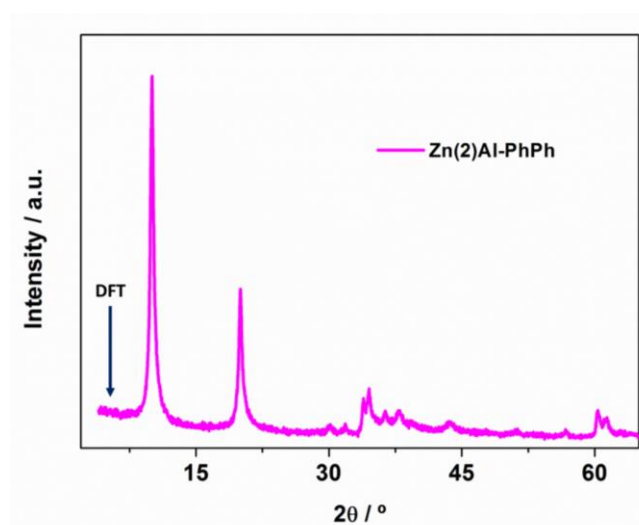


Figure 5: Experimental XRD pattern of Zn(2)Al-PhPh and indication of the 2θ angle of the first peak predicted by DFT.

The difficulty to intercalate PhPh can be supported by the unfavorable substitution energy in the LDHs' interlayers calculated in this work for phenolphthalein (+ 0.5 eV), relatively to the nitrate anion present in the precursor Zn(2)Al-NO₃ material, the hydroxide anions produced during the calcination-rehydration step (- 1.2 eV), or the carbonate anions existing in hydrotalcite (- 1.9 eV) which was also tested in this work.

Nevertheless, it is possible to verify the presence of PhPh, according to FTIR (not shown) and UV-Vis measurements, which should be an indication of its immobilization on the LDH surface. The detection of PhPh on the LDH surface may be supported by a favorable adsorption energy of PhPh onto the LDHs' Zn(2)Al surface, with an adsorption energy in the order of magnitude typically associated with chemisorption of organic molecules. However, the obtained material may still have some amount of physically adsorbed material to release the functional anion in a controlled manner under electrolyte

conditions which favor metallic corrosion, as demonstrated by the release profile of LDH-PhPh in 0.05 M NaCl presented below.

Phenolphthalein silica nanocapsules and thymol blue chitosan microcapsules

From SEM data presented in Figure 6 it is possible to observe that phenolphthalein silica capsules have a spherical and fairly regular shape with sizes comprised between 300 and 700 nm while chitosan microcapsules show spherical shape and sizes in the micrometer range (between 2 and 6 μm).

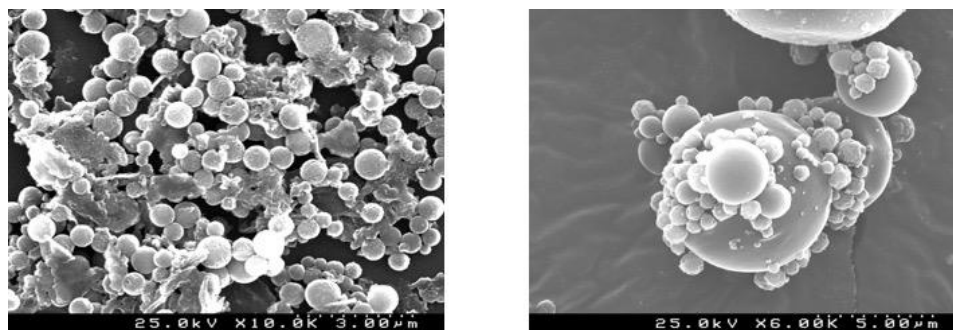


Figure 6: SEM pictures of (left) silica nanocapsules with PhPh and (right) chitosan microcapsules with TB.

Figure 7 shows the release profiles of PhPh from LDH-PhPh and TB from chitosan microcapsules in 0.05 M NaCl solution. The results reveal a differentiated release of indicators, with chitosan microcapsules releasing most of TB within the first 4 hours (ca. 75 % of total loading) while in the case of LDH-PhPh only 15 % of PhPh is released during the monitored time.

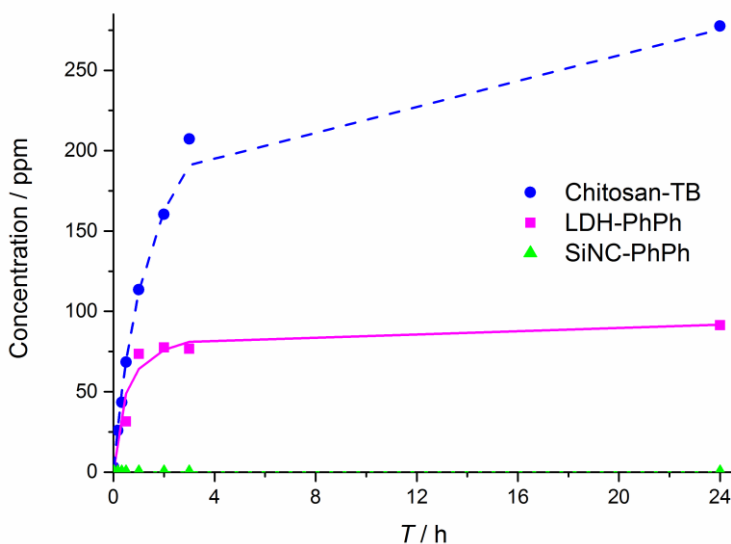


Figure 7: Release profiles of PhPh from layered double hydroxides and TB from chitosan capsules in 0.05 M NaCl.

Regarding the release of phenolphthalein from silica nanocapsules (SiNC), the amount released in NaCl 0.05 M, is below the detection limit of the spectrophotometer, which did not allow the quantification of the released material. Therefore, it is assumed that, up to 24 h, there is no release of phenolphthalein from silica nanocapsules.

SIET measurements and visual detection of corrosion

The materials prepared and characterized in the previous section were used directly in solution to detect corrosion activity in different metal systems, namely Zn-Fe, Al-Cu and also in magnesium alloy AZ31. Figure 8 shows the pH maps obtained by SIET and the corresponding optical images in the presence of some of the additives above described. As expected, the galvanic coupling of dissimilar metals such as Zn-Fe and Al-Cu leads to a polarization of the different electrodes according to the electrochemical series: Zn acts as anode and Fe as a cathode when electrically connected, while in the case of Al-Cu system Al is the polarized positively and Cu negatively. The consequence of this polarization is the occurrence of the reduction process in the cathode which results in a raise of pH near its surface. In both systems LDH-PhPh was able to change color, consistent with the properties of the pH indicator immobilized (color transition from colorless to pink).

In the case of magnesium alloy AZ31, Mg readily reacts with H₂O causing a significant raise in pH across the whole surface. The pH indicator TB, which is released in a significant extent as soon as it is in contact with water, causes a sudden change of the color solution (yellow to blue).

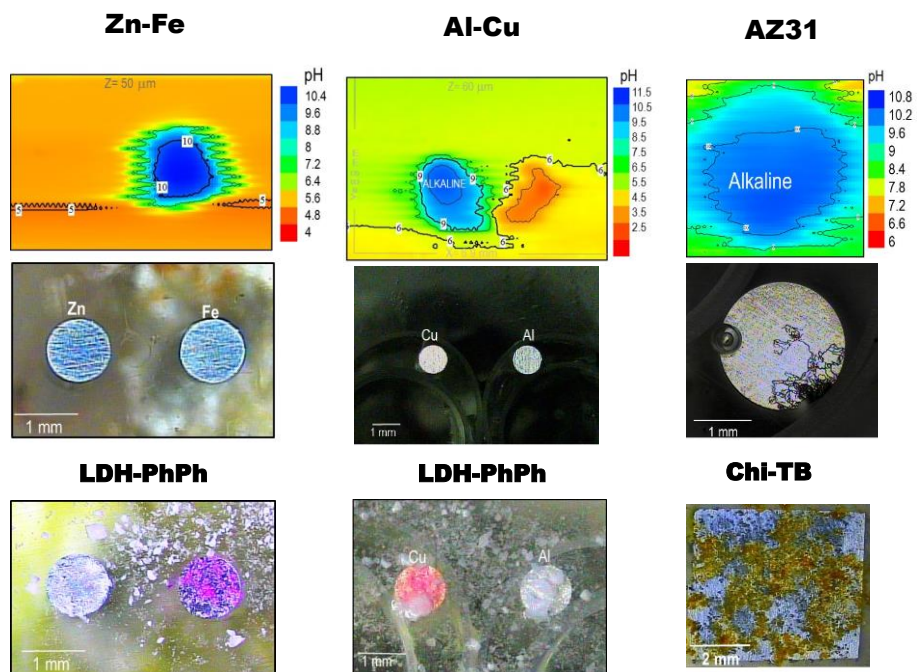


Figure 8: SIET maps and optical images of the Zn-Fe, Al-Cu and AZ31 systems acquired in 0.05 M NaCl solution in the presence of different sensing additives.

CONCLUSIONS

In this work different inorganic and organic materials were synthesized to be used as carriers for pH indicators phenolphthalein and thymol blue. These materials display differentiated structure, morphology and size. Layered double hydroxides are plate-like materials with dimensions in the

nanometer range, whereas silica mesoporous capsules show sizes within the sub-micron range and chitosan capsules in the micrometer range. Among the three systems, chitosan microcapsules shows the most extensive release of indicator, whereas for silica nanocapsules the indicator is not released under the studied conditions.

The obtained materials were tested directly in solution in the presence of different metals. The results show a correlation between the rise in pH due to cathodic reactions and changes in the color of the pH indicator. As a result, these materials show features that can be suitable for development of coatings for corrosion sensing.

ACKNOWLEDGEMENTS

Thanks are due to J. R. B. Gomes and C. S. Neves for supervising the computational work and the AFM results, respectively. SMARCOAT - This project has received funding from the European Union's Horizon 2020 research and innovation programme under the Marie Skłodowska-Curie grant agreement No 645662. JT thanks FCT for the research grant IF/00347/2013. The computational work was financed in the framework of Projecto 3599 - Promover a Produção Científica e Desenvolvimento Tecnológico e a Constituição de Redes Temáticas (3599-PPCDT) e participado pelo Fundo Comunitário Europeu FEDER.

REFERENCES

1. J. Zhang, G. S. Frankel, "Corrosion-Sensing Behavior of an Acrylic-Based Coating System," *Corrosion*, 55 (1999): p 957.
2. I. M. El-Nahal, S. M. Zourab, N. M. El-Ashgar, "Encapsulation of phenolphthalein pH-indicator into a sol-gel matrix," *J. Dispersion Sci. Technol.*, 22 (2001): p. 583.
3. W. Li, L. M. Calle, "Controlled release microcapsules for smart coatings," *NACE Corrosion 2007*, Paper 07228 (Nashville, TN).
4. F. Maia, J. Tedim, A. C. Bastos, M. G. S. Ferreira, and M. L. Zheludkevich, "Active sensing coating for early detection of corrosion processes," *RSC Adv.*, 4 (2014): p. 17780.
5. J.-H. Choy, J.-S. Jung, J.-M. Oh, M. Park, J. Jeong, Y.-K. Kang, and O.-J. Han, "Layered double hydroxide as an efficient drug reservoir for folate derivatives," *Biomaterials*, 25 (2004): p. 3059.
6. M. F. Montemor, D. V. Snihirova, M. G. Taryba, S. V. Lamaka, I. A. Kartsonakis, A. C. Balaskas, G. C. Kordas, J. Tedim, A. Kuznetsova, M. L. Zheludkevich, M. G. S. Ferreira, "Evaluation of self-healing ability in protective coatings modified with combinations of layered double hydroxides and cerium molybdate nanocontainers filled with corrosion inhibitors," *Electrochim. Acta*, 60 (2012): p. 31.
7. J. Tedim, A. Kuznetsova, A. N. Salak, F. Montemor, D. Snihirova, M. Pilz, M. L. Zheludkevich, M. G. S. Ferreira, "Zn-Al layered double hydroxides as chloride nanotraps in active protective coatings," *Corros. Sci.*, 55 (2012): p. 1.
8. K. Qian, T. Shi, S. He, L. Luo, X. liu, Y. Cao, "Release kinetics of tebuconazole from porous hollow silica nanospheres prepared by miniemulsion method," *Microporous Mesoporous Mater.*, 169 (2013): p. 1.
9. I. Sousa, F. Maia, A. Silva, Â. Cunha, A. Almeida, D. V. Evtuyugin, J. Tedim, M. G. Ferreira, "A novel approach for immobilization of polyhexamethylene biguanide within silica capsules," *RSC Adv.*, 5 (2015): p. 92656.
10. J. Carneiro, J. Tedim, M. G. S. Ferreira, "Chitosan as a smart coating for corrosion protection of aluminum alloy 2024: A review," *Prog. Org. Coatings*, 89 (2015): p. 348.

11. A.K. Covington, *Acid-base indicators, in Indicators*, Ed. E. Bishop, New York, NY: Pergamon Press, 1972, p. 16 (Appendix 8).
12. F. Maia, J. Tedim, A.C. Bastos, M.G.S. Ferreira, M.L. Zheludkevich, "Nanocontainer-based corrosion sensing coating," *Nanotechnology*, 24, 41 (2013): p. 415502.
13. P. Giannozzi, S. Baroni, N. Bonini, M. Calandra, R. Car, C. Cavazzoni, D. Ceresoli, G. L. Chiarotti, M. Cococcioni, I. Dabo, et al. "QUANTUM ESPRESSO: a modular and open-source software project for quantum simulations of materials.," *J. Phys. Condens. Matter*, 21 (2009): p. 395502.
14. T. L. P. Galvão, C. S. Neves, A. P. F. Caetano, F. Maia, D. Mata, E. Malheiro, M. J. Ferreira, A. C. Bastos, A. N. Salak, J. R. B. Gomes, J. Tedim, M. G. S. Ferreira, "Control of crystallite and particle size in the synthesis of layered double hydroxides: Macromolecular insights and a complementary modeling tool.," *J. Colloid Interface Sci.*, 468 (2016): p. 86.
15. J. P. Perdew, K. Burke, M. Ernzerhof, "Generalized Gradient Approximation Made Simple," *Phys. Rev. Lett.*, 77 (1996): p. 3865.